

## Computational Flow Analysis of Para-rec Bluff Body at Various Reynold's Number

**B. Kaleeswaran<sup>(1#)</sup>, S. Aravind<sup>(2#)</sup>, B. Ganesh<sup>(3#)</sup> and S. Sougathali<sup>(4#)</sup>**

<sup>(1#)</sup>*M.Tech (CFD) – University of Petroleum and Energy Studies,  
Uttarakhand, Dehradun, India.*

<sup>(2#)(3#)</sup>*M.E (Aeronautical Engineering) – Karpagam University - Coimbatore, India.*

<sup>(4#)</sup>*M.E (CAD/CAM) – Central Institute of Plastic Engineering and Technology  
Chennai, India.*

### Abstract

This project is about the computational flow analysis of Para-rec bluff body at various Reynolds number. This flow analysis were based on Reynold's number modifications and were analysed in a medium at various turbulent flows by using an available CFD software Ansys-Fluent© 14.5 version. This analysis was used to find out the drag coefficients of the model. Based on the results obtained after analysing the conclusion was drawn. The solid medium and liquid medium for this flow analysis was to be taken as steel and water.

**Keywords:** Bluff body; Computational flow; Drag coefficients; Reynolds number; Turbulent flows; Ansys-Fluent©.

### 1. Introduction

Computational flow involves the study of an object under moving condition. In this paper computational flow of para-rec bluff body was analysed at different Reynold's number to determine the pressure drag and also the drag coefficients. This study would help scientists and researchers to know about the importance of the para-rec shape objects and its usefulness in designing a new type of re-entry vehicles.

## 2. Literature Survey

The literature survey for this paper is taken from highly reputed papers and books and is summarized as follows. From the Fluid Mechanics book by David.C.Wiggert and Merle Potter of Schaum's Series [1].The flow analysis involves studying external flows ranging from low Reynold's number flows to high Reynold's number flows.Flow over a bluff body model involves region of separation with recirculation zones, region with high viscosity called wakes [2]. Laminar Boundary layer exists near to the object in the case of low Reynold's number flows and the flow separation decreases as Reynold's number increases. An in viscid flow occurs near to the stagnation point and upto front part of the bluff body. Reynold's number flows for cases  $<5$  is termed as Stokes flow [3]. Increase in Reynold's number cases transition flow to occur. High Reynold's number flows causes turbulent flows to occur which pushes the region of separation still to the rear.

During the Reynold's number flows from low to medium the value of CD remains high.But,when the flow reaches the Reynold's number of  $3 \times 10^5$  the transition state occurs from laminar to turbulent. As a result of this the turbulent boundary layer gets attached to the body so firmly and this results causes the separation to occur totally at the rear side of the object leading to increased pressure drag and increased CD.[Source: Fundamentals of Aerodynamics by J.D.Anderson]

## 3. Designed Model

This model was designed on the idea, that is parabolic curved front part is attached with rectangular rear part (Para-rec). The model designed above fig.3.1 shows the grid formation around the Para-rec model with its shape designed. The model was designed using Gambit ® with a parabolic curve of radius 0.5 m and with rear part rectangular length of 0.5 m.

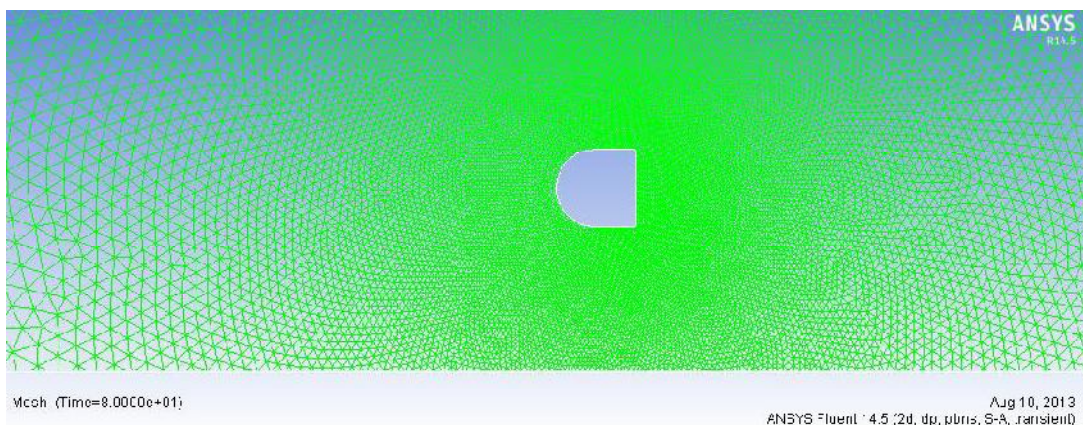


**Fig. 3.1:** Mesh grid of the parabolic front part and rectangular rear part body (Para-rec).

#### 4. Equations Used

This model was solved with three major equations; Continuity equation; and Momentum equation; [Source: Introduction to CFD by J.D.Anderson].

##### 1. Continuity equation

$$\frac{d\rho}{dt} + \nabla \cdot (\rho V) = 0 \quad (4.1)$$

##### 2. Momentum equation

X axis:

$$\partial \frac{\rho U}{\partial t} + \nabla \cdot (\rho u V) = - \frac{\partial p}{\partial x} + \frac{\partial \tau_{xx}}{\partial x} + \frac{\partial \tau_{xy}}{\partial y} + \frac{\partial \tau_{xz}}{\partial z} \quad (4.2)$$

Y axis:

$$\partial \frac{\rho V}{\partial t} + \nabla \cdot (\rho v V) = - \frac{\partial p}{\partial y} + \frac{\partial \tau_{xy}}{\partial x} + \frac{\partial \tau_{yy}}{\partial y} + \frac{\partial \tau_{yz}}{\partial z} \quad (4.3)$$

Z axis:

$$\partial \frac{\rho W}{\partial t} + \nabla \cdot (\rho w V) = - \frac{\partial p}{\partial z} + \frac{\partial \tau_{xz}}{\partial x} + \frac{\partial \tau_{zy}}{\partial y} + \frac{\partial \tau_{zz}}{\partial z} \quad (4.4)$$

#### 5. Inputs Given

##### 5.1. Mesh Consideration

For this 2D model tri pave mesh was used as it was found to produce good fine mesh in the near vicinity regions. As the model is of bluff body shape using a structured mesh is of difficult and also the vector plots obtained with structured mesh would not yield good results. Moreover making a structured mesh for such geometries is a time consuming and it increases the mesh size too. A mesh interval size of 0.01 was considered in Gambit. This tri-pave mesh arrangement can reduce the skewness factor to large amount in the case of complex geometries.

##### 5.2. Initial Conditions and Solver Settings

The mesh file was saved after giving the boundary conditions and exported as 2DDP mesh to the Ansys Fluent Solver version 14.5[5], a commercially available FVM based solver.

##### 5.3. Boundary Considerations

The boundary conditions were designed as follows.

**Table 5.1:** Boundary Conditions.

S. No	Boundary Conditions	Edges Taken
1.	Wall	Model- the designed 2D profile of the object
2.	Wall	Top and Bottom edges of the far field
3.	Velocity Inlet	Front vertical edge of the far field
4.	Outflow	Back vertical edge of the far field

## 6. Results and Discussion

In this sectional part various contour plots and velocity vector plots obtained with varying Drag curves and XY Plots were discussed.

1. Velocity Contour Plots.
2. Pressure Contour Plots.
3. Vector Plots.
4. Drag Curves.

As various plots were obtained in this study it would be not sufficient to put all the approximate 78 contour plots in this paper. Thus, Re number flows at greater than  $3 \times 10^6$  that is  $5.95 \times 10^6$  model was only referred in figure as it produces high turbulence effects.

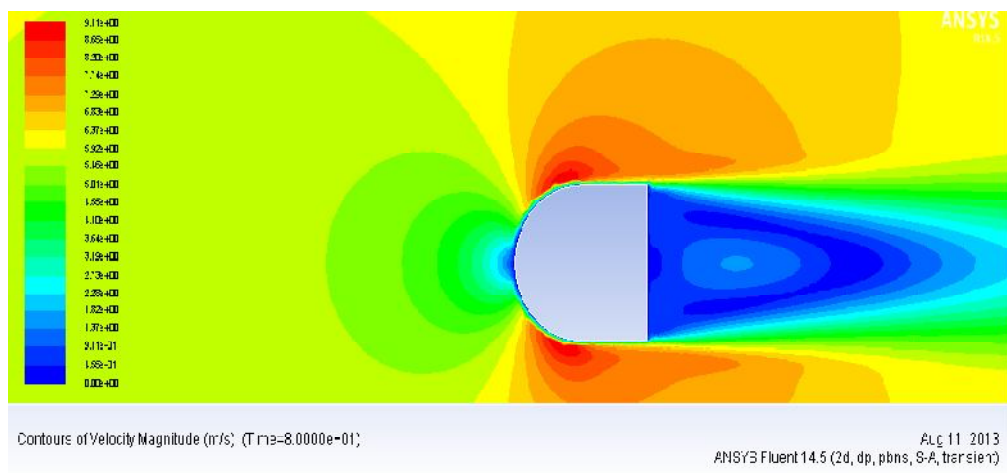


**Fig. 6.1:** Velocity Contour plot over the Para-rec model at very high Re number.

The fig.6.1.shows the velocity contour plot over the Para-rec model at a very high Reynold's number of  $5.95 \times 10^6$ . A region of less velocity was found near to the stagnation point and at the rear part of the model. But near to the parabolic and rectangle joining areas there occurs a region of high velocity.

The diagram shown below gives the pressure contour plot of the Para-rec model at a high Reynold's number. There occurs a region of very high pressure at the front due to stagnation region and the pressure reduces at the aft due to movement of fluid from a region of high pressure to a region of low pressure(Bernoulli's Principle).There occurs evidence of attachment of flow at the rear part of the body as one could see a region of less pressure of blue patch region at the corners.

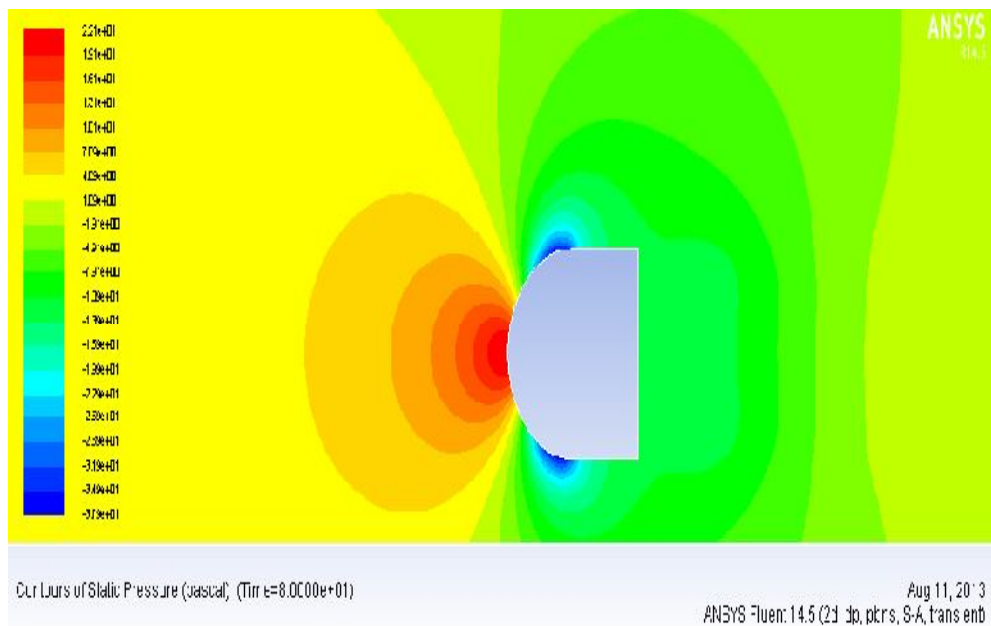


**Fig. 6.2:** Pressure Contour plot over the Para-rec model at very high Re.

### 7. CD Plots

A combined CD plot of the model was produced to obtain the main idea of the results. Thus, CD plots of this model ranging from Re 995000, 2985643 to 5971286 was obtained to study the results.

These CD plots were calculated based on Force formula that is;

$$F = \frac{1}{2} \cdot \rho \cdot v^2 \cdot L \cdot CD \tag{7.1}$$

The force normally obtained was the pressure force along <1, 0, 0> plane and was used in the formula (7.1) to obtain the CD values.

From the table 7.1, the decrease in the value of CD with the increase in the value of Reynold's number was clearly visible to this model. It was found that the Para-rec models possess heavy drag.

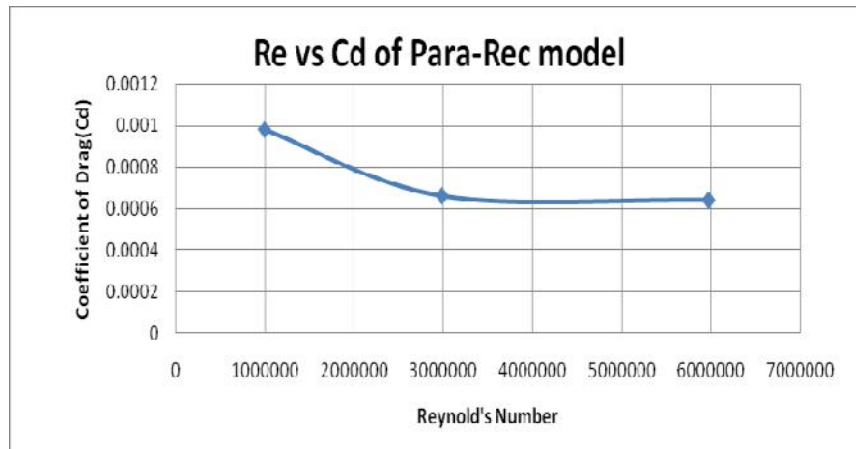


**Fig. 7.1:** Re vs CD plot of the Para-Rec model at Various Re Numbers.

From the fig.7.1.the CD values of the Para-Rec model decreases with increase in the Reynold's number. The region of flow separation also varies. This is due to variation of the reattachment of the flows to the body surface.

## 8. Conclusion

For this model with varying Reynold's number simulations were done to obtain the CD values. For  $Re < 10^6$  medium Reynold's number, flow is attached and streamlines are found to be symmetrical. For  $Re < 3 \times 10^6$  but not lesser than  $10^5$  the flow becomes separated but it tries to attach to the body at the backend. For  $Re > 3 \times 10^6$  ( $5.97 \times 10^6$ ) there occurs flow separation at the front side of the object itself due to high Reynold's number. This is due to the formation of the turbulent flows. But, in the last case the value of CD reduces due to less region of separation than other cases.

For this CFD analysis unsteady flow analysis were done for different Reynold's number cases. For medium Reynold's number case and high Reynold's number cases the flow was considered to be as transient with varying velocities and with steady densities and viscosities. Spalart's Alamaras Turbulence model was chosen to analyse and capture high turbulent stagnation regions and the separation regions of the flow. The main idea of this paper is to find the drag coefficients of the model at different Reynold's number as this couldn't be found using a wind tunnel analysis. Even if wind tunnel is used the cost would be much higher when compared to CFD analysis. From the plots and graphs it was understood that the flow separation is higher in the case of Para-Rec model. From the results, Para-Rec or semi cylinder model produces high drag and is suitable for Re-entry cases.

## **References**

- [1] Merle Potter, David.C.Wiggert (1986). Fluid Mechanics. 2nd ed. Newyork: Schaum's series. Pg. 156-176.
- [2] W.C.L.Shih, C.Wang, D.coles and A.Roshko (1993), Experiments on flow past rough circular cylinders at large Reynolds numbers. Journal of wind engineering and industrial aerodynamics.
- [3] John C K Cheung, William H Melbourne, Effects of surface roughness on a circular cylinder in supercritical turbulent flow, Department of Mechanical Engineering, Monash University.
- [4] Pijush.K.Kundu, Ira M.Cohen (2002). Fluid Mechanics. New York: Academic Press. Pg.256-300.
- [5] Fluent 14.5. Available: [www.sharcnet.in](http://www.sharcnet.in). Last accessed 20<sup>th</sup> July 2013.
- [6] J.D.Anderson (1998).Fundamentals of Aerodynamics. New Delhi: Tata McGraw Hill Publications.Pg.348-352.

